

Supplement

# Aerosol Effective Radiative Forcing in the Online Aerosol Coupled CAS-FGOALS-f3-L Climate Model

Hao Wang <sup>1,2,3</sup>, Tie Dai <sup>1,2,\*</sup>, Min Zhao <sup>1,2,3</sup>, Daisuke Goto <sup>4</sup>, Qing Bao <sup>1</sup>, Toshihiko Takemura <sup>5</sup>, Teruyuki Nakajima <sup>4</sup> and Guangyu Shi <sup>1,2,3</sup>

<sup>1</sup> State Key Laboratory of Numerical Modeling for Atmospheric Sciences and Geophysical Fluid Dynamics, Institute of Atmospheric Physics, Chinese Academy of Sciences, Beijing 100029, China; wanghao@lasg.iap.ac.cn (H.W.); zhaomin@lasg.iap.ac.cn (M.Z.); baoqing@lasg.iap.ac.cn (Q.B.); shigy@mail.iap.ac.cn (G.S.)

<sup>2</sup> Collaborative Innovation Center on Forecast and Evaluation of Meteorological Disasters/Key Laboratory of Meteorological Disaster of Ministry of Education, Nanjing University of Information Science and Technology, Nanjing 210044, China

<sup>3</sup> College of Earth and Planetary Sciences, University of Chinese Academy of Sciences, Beijing 100029, China

<sup>4</sup> National Institute for Environmental Studies, Tsukuba 305-8506, Japan; goto.daisuke@nies.go.jp (D.G.); nakajima.teruyuki@nies.go.jp (T.N.)

<sup>5</sup> Research Institute for Applied Mechanics, Kyushu University, Fukuoka 819-0395, Japan; toshi@riam.kyushu-u.ac.jp

\* Correspondence: daitie@mail.iap.ac.cn; Tel.: +86-10-8299-5452

## S1 SSA

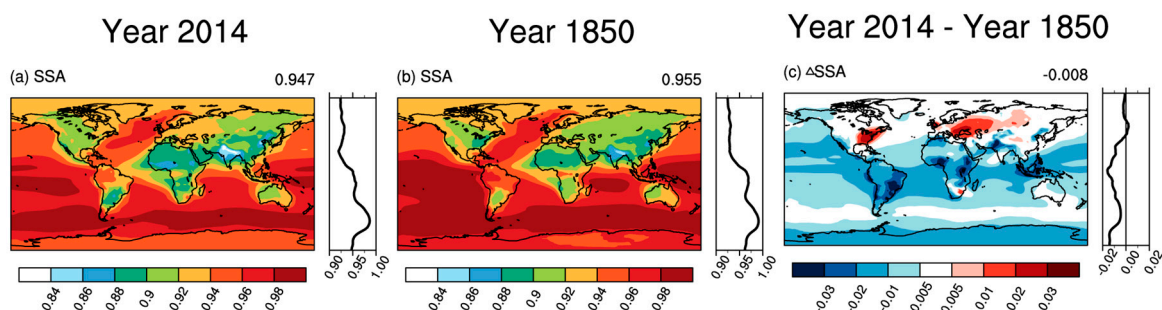


**Figure S1.** The modelled annual mean single scatter albedo (SSA) in the year 2014 (a), year 1850 (b), and the year 2014-1850 (c). The zonal means plot is located in the right of each subplot. The global mean value is shown the top right corner of each map.

Figure S1 shows the distribution of the single scatter albedo (SSA) for the year 2014, 1850, and the difference between the year 2014 and 1850. The SSA occurs higher in the ocean and lower in the land due to the sea salt dominated in the ocean and various type aerosols dominated in the land. The increase of SSA over the Europe and eastern America is possibly caused by the increase of sulfate. The decrease of SSA over the center Africa is possibly caused by the increase of carbonaceous.

## S2 Precipitation

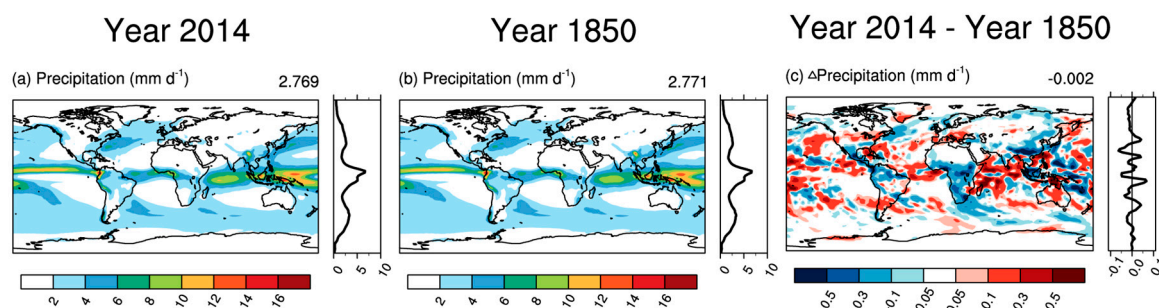


**Figure S2.** The same as Figure S1, but for precipitation.

Figure S2 shows the distribution of the precipitation for the year 2014, 1850, and the difference between the year 2014 and 1850. The precipitation occurs higher within equatorial regions. The decrease of precipitation over the East Asia is possibly caused by the increase of aerosols. Globally, the precipitation has also been a slight decline with the values of  $-0.002 \text{ mm d}^{-1}$ .

### S3 High, Medium and Low Cloud Fraction

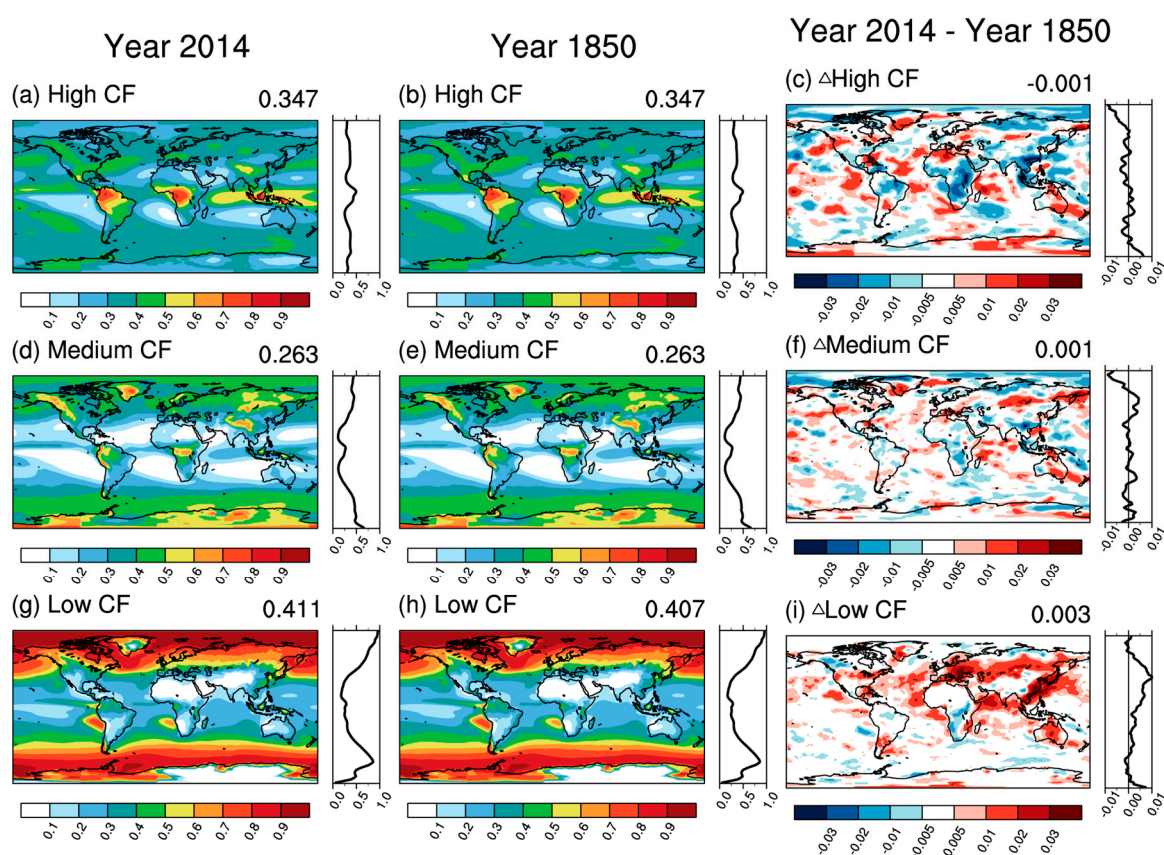


**Figure S3.** The modelled annual mean cloud fraction (CF) in the year 2014 (left), year 1850 (middle), and the year 2014-1850 (right). The zonal means plot is located in the right of each subplot. The global mean value is shown in the top right corner of each map. The first row (a, b, c) is high cloud fraction (High CF), the second row (d, e, f) is medium cloud fraction (Medium CF), and the last row (g, h, i) is low cloud fraction (Low CF).

Figure S3 shows the distribution of the cloud fraction for the year 2014, 1850, and the difference between the year 2014 and 1850. The changes of low cloud fraction are largest among the three types cloud. The relatively significant increasing of low cloud fraction over the East Asia and Europe is possibly caused by the increase of aerosols.



© 2020 by the authors. Licensee MDPI, Basel, Switzerland. This article is an open access article distributed under the terms and conditions of the Creative Commons Attribution (CC BY) license (<http://creativecommons.org/licenses/by/4.0/>).